IoT Project Report: Localization system based on UWB Qorvo QM33120WDK1 development kit

Paolo Golinelli, 247450

***Abstract*—This project report presents the development of a localization platform based on the QM33120WDK1 development kit from Qorvo, with an emphasis on applications in the field of Internet of Things (IoT). More specifically, the report details the design and implementation of the system's ranging and communication capabilities, which leverages Ultra-Wideband (UWB) technology for precise positioning, and the fusion of data through the implementation of a Kalman Filter (KF). Additionally, it covers the development of a web-based visualization tool that enables real-time monitoring of the estimated positions, and the establishment of a structured dataset for efficient storage and organization of measurement information. Finally a brief discussion on the system's localization performance is made.**

I. Introduction

LOCALIZATION systems play a critical role in the evolving field of Internet of Things (IoT) applications, enabling devices to understand and interact with their surrounding environment. Accurate and reliable real-time positioning of a multitude of nodes is essential not only in domestic scenarios, such as smart homes where location-aware automation can be used for enhancing the interaction capabilities of humans and smart appliances, but also in Industrial IoT (IIoT) settings where precise product's and vehicles tracking can improve process planning and optimization, and safety monitoring.

Despite the advancements in localization technologies, a key challenge remains: achieving accurate real-time localization with minimal setup cost and complexity. Designing an effective positioning system requires addressing the trade-off between performance, cost, and feasibility. The difficulty arises from the fact that there is no unique solution: such a system can be engineered for high precision using specialized hardware, at the cost of increased complexity and economic budget, or, conversely, it can prioritize simplicity and low cost, often sacrificing accuracy but gaining in scalability.
The choice of localization technology, hardware platform, and communication protocol significantly influence the system's capabilities and limitations. Hence, the solution to the trade-off is to make informed decisions on which technologies to adopt in order to balance technical requirements with practical constraints like deployment cost, ease of integration, and environmental robustness.

The problem of localization and tracking is common to a multitude of fields, and it is solved following a lot of different approaches, with the two main being vision systems and radio-based localization systems. The latter is based on the exchange of one or more signals between two antennas, in order to retrieve either the distance between them or the angle at which the signal arrives and/or departs. The most common approach for distance measurements is Time of Flight (ToF) which basically means to measure the time the signal took while traveling between the receiver and the transmitter. In practice, most often a round-trip approach is implemented, called Two Way Ranging (TWR) [1], where a signal is exchanged back to the initial transmitter, removing the need of synchronization of clocks. Instead, for angle measurement the main idea involves a set of antennas at the receiving end, which will receive the signal at slightly different times according to the incoming signal angle, allowing to measure the Angle of Arrival (AoA) [2]. Since the spatial difference between the receiving antennas is very limited, in practice the angle is estimated by measuring the Phase Difference of the received signals (PDoA).

Common technologies used for radio-based localization, are Ultra-Wideband (UWB) [3], Bluetooth Low Energy (BLE) [4], Wi-Fi [5], and Zigbee [6]. Each leverages different signal characteristics to estimate the distance or angle between devices. UWB is known for its high-precision ranging, typically measuring ToF or AoA, and offers centimeter-level accuracy with low latency and low interference, making it ideal for indoor positioning in both industrial and smart home environments. However, UWB hardware can be more expensive and power-intensive. BLE and Wi-Fi, on the other hand, are more available and affordable, often using Received Signal Strength Indicator (RSSI) for coarse localization, but they suffer from multi-path effects and signal instability, resulting in very poor accuracy [7].
What differentiates UWB technologies over traditional methods is the use of signals covering a wide frequency spectrum. In fact, wide bandwidth signals are less affected by multi-path situations and show greater penetration, allowing to work even in the presence of obstacles, and interfering equipment.

Another important aspect requiring careful decision making in the design step regards the observability of the states, i.e. the ability to retrieve sufficient information to fully describe the states of the system. In the context of multi-node localization, observability is achieved when only a single configuration of the nodes satisfy the measurement constraint.

In such a system observability mainly depends on the number of fixed anchors [8], and availability of measurements. When measuring distance, triangulation is possible using at least three fixed anchors measuring the node simultaneously in $2D$ problems [9], and four anchors in $3D$. Instead, with just two anchors measuring AoA a unique node position is determined both for $2D$ and $3D$ problems [10], although tridimensional angle measurements usually comprise of both azimuth and elevation angle, which basically consist of two measurements. It can be easily proven that, by the combination

of distance and angle measurement a unique node position is determined even with as little as one fixed anchor. But most systems use a broader set of states than just the position of the nodes. For example it is common for wheeled robots to include the heading (pitch) as a state, and when the dynamic of the system cannot be neglected it is necessary to include velocity or even acceleration in the set of states. In such systems a single position measurement alone is not enough to observe all states [11]. This explains the need of dynamic estimators, like the KF, which are estimation algorithm that fuse the dynamic of the system with the measurements taken over time to gain information on the full set of states.

Contributions: This project proposes a minimal-setup centralized localization system using a single anchor equipped with UWB hardware capable of retrieving both AoA and ToF measurements. By combining this with a Kalman Filter, we aim to achieve real-time, low-cost, and scalable localization suitable for indoor environments.

Having a single anchor allows the system to be essentially plug-and-play, thanks to the fact that no precise positioning of anchors or careful calibration procedure is required. As previously discussed one solution to achieve observability of the node's position given a single absolute reference is to retrieve both distance and angle measurements at the side of the fixed anchor. Moreover, to gain information on the velocity of the nodes, and to achieve resiliency to uncertainty of measurements, a simple KF scheme is implemented. In fact the KF leverages measurement uncertainty to obtain the most optimal estimate possible given the available information.
The decision for the measurement system verted to the Qorvo QM33120WDK1 development kit [12], as it is based on the Ultrawide Bandwidth (UWB) technology to obtain precise distance and angle measurement. Since the kit is specifically designed for IoT applications it provides developers with the necessary hardware and software tools to build scalable, high-precision localization systems.

In summary the main contributions of this work are:

- Implementation of a centralized localization system using only a single UWB anchor with AoA and ToF.
- Real-time data acquisition, parsing, and processing from Qorvo UWB sensors.
- Application of a Kalman Filter for noise reduction and smooth tracking.
- Real-time visualization dashboard implemented using Node-RED.
- Integration of a time-series DB for persistent storage.
- Design of a validation campaign using a motion capture (MoCap) system for performance assessment.

The rest of the paper is organized as follows. In Section-II the Related Work on the subject is reviewed. Section III briefly details the problem statement and the system layout. Section-IV presents the sensing technology both in terms of hardware and in configuration. Then the architecture and the software logic is laid out in Section-V, subdivided between functional layers. Follows in Section-VI the description and results of the performance evaluation. Finally Section-VII wraps up the report, detailing the conclusions of the presented work.

II. Related Work

The problem of localizing a set of nodes using UWB ranging measurements is most commonly solved in the literature through multi-anchors systems. Numerous works make use of the Extended KF (EKF) to fuse data coming from ranging sensors with the information provided from Inertial Measurement Units (IMU) [13], [14], benefiting from the high number of available measurements to obtain high tracking accuracy, improved robustness to interference, and resilience to modeling errors.

In contrast, single-anchor systems present a significantly more challenging scenario to be solved, due to reduced observability and scarcity of data. While inevitably achieving worse performances, the literature covering the problem is rich of innovative and interesting solutions.

The work by Großwindhager and Rath et al. (2018) [15] introduces a single-anchor, multi-hypothesis system capable of localizing multiple tags. A key innovation of their framework is the use of virtual anchors generated from multipath reflections, enabling enhanced localization performance without requiring multiple physical anchors. This method assumes prior knowledge of the indoor environment's floor plan, which requires a non-negligible deployment effort, but still minimizing the infrastructure cost and setup time.

An important contribution in the field of single-anchor tracking is presented by Cao et al. (2020) [16], who developed a system that combines a single UWB ranging anchor with measurements from a 9-axis IMU, using an EKF for data fusion. A key innovation of their work is the estimation of the device's velocity, obtained by analyzing the radial change across three successive UWB ranging measurements. This additional velocity estimate renders the otherwise unobservable system temporarily observable. Their approach demonstrated a reduction in tracking error of up to 60%, proving to be effective in accurate tracking of mobile agents equipped with UWB TWR modules and low-cost IMUs, all while relying on a minimal infrastructure that supports easy scalability.

In the field of distributed robotics single anchor localization is commonly dealt by also retrieving relative measurements between agents alongside the absolute measurements to the fixed reference. Riz et al. (2023) [9] discuss challenges in ensuring spatial distinguishability when trilateration is performed with non-simultaneous measurements, highlighting how possible ambiguities might arise. In Roumeliotis and Bekey publication (2002) [17] which first laid out the well established Interim Master Cooperative Localization algorithm, it is shown how observability can be obtained for three robots measuring intermittent inter-agent distances given that one robot remains stationary, basically acting as a fixed reference.

A more hardware-driven solution is to achieve full observability with just a single measurement. In the case of heading-invariant tags this is achieved by measuring both the distance and the angle of arrival at the side of the anchor. Wang et al. (2020) [18] provides design guidelines for decimeter-level accuracy and high-efficiency multi-agent centralized localization system. In particular they provide a detailed analysis on

how to limit message exchanges while performing a two-way ranging measurement via UWB technology.

The approach adopted in this project follow the latter paradigm. Specifically, it leverages both angle and distance measurement from a single UWB anchor equipped with a dual-antenna transceiver to track multiple tags. The system simplifies many aspects compared to the state of the art, for instance, by exclusively relying on infrastructure-based AoA plus ToF measurements and excluding IMUs, inter-agent measurements, or reflection modeling, it favors a lightweight and rapid implementation.

While this work does not propose a novel contribution, it validates a tracking system with limited requirements, which integrates existing technologies, such as Node-RED, InfluxDB, and Kalman filtering, into a working system. The obtained results demonstrate that even with limited hardware and no prior calibration of the environment, acceptable tracking performance can be achieved.

III. Description of the work

A. Problem statement

The main problem addressed in this work is the design of an indoor localization system capable of tracking multiple mobile nodes (tags) in real time, using only a single fixed anchor. Traditional systems often require multiple anchors to achieve good accuracy and observability, but such setups involve significant installation effort, calibration, and infrastructure.
To reduce this complexity, the goal is to use an absolute reference node capable of measuring both distance (ToF) and azimuth angle (AoA), and to combine these noisy observations over time using a KF to estimate position and velocity of each mobile tag. The final system should be plug-and-play, suitable for IoT environments, and able to visualize position and movement both in real-time, and in replay mode, by loading historic data from a database.

In Fig. 1 the overall system is displayed highlighting the employed devices, communication and measurement lines and the reference frame.

B. System overview

The developed system is composed of the following layers:

- Sensing Layer: a Qorvo UWB anchor node communicates with each mobile tags to measures both ToF and AoA.
- Acquisition Layer: a real-time data stream is established between the anchor and a local processing unit via USB communication.
- Processing Layer: raw data is parsed, structured, and filtered using a KF to estimate smoothed tag positions.
- Storage Layer: A time-series database stores position history for further analysis and replay.
- Visualization Layer: A Node-RED-based dashboard visualizes the tag positions in real-time and in replay mode, including historical trajectories, and provides configuration options for localization parameters.
- Validation Layer: The system will be validated using a Motion Capture (MoCap) ground truth to assess performance.

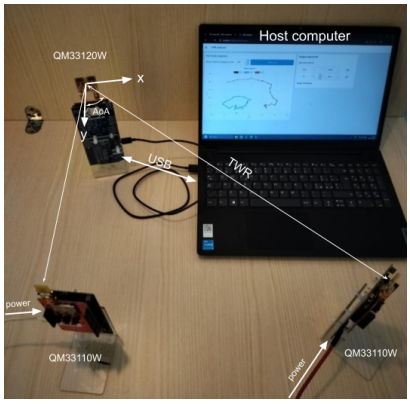

Fig. 1: System setup and communication flow.

The full Node-RED flow, firmware binaries and the data and code for analyzing the system performance are available at: https://github.com/PaoloGolinelli/UWBlocalization

IV. Measurement Unit and Sensing Architecture

This section details the sensing layer of the system, describing the employed hardware, its configuration, and the communication interface.

The measurement unit is based on the Qorvo *QM33120WDK1* development kit, which combines the *Nordic nRF52840 DK* microcontroller evaluation boards with UWB transceivers from the QM33xx family. Each evaluation board features an *nRF52840 SoC* equipped with an integrated BLE radio, USB interface for power and serial communication, and an on-board J-Link debugger for firmware flashing and diagnostics.
The UWB transceivers used include:

- **QM33120W**: Equipped with a dual-antenna array, capable of computing both Time of Flight (ToF) and Angle of Arrival (AoA) using Phase Difference of Arrival (PDoA). This board is used as the *fixed anchor*, and assumes the role of the measurement initiator.
- **QM33110W**: Equipped with a single antenna and capable of ToF-based ranging only. These are used as the *mobile tags* to be localized; they are the responder in the measurement.

The transceivers exchange UWB signals to perform Two-Way Ranging (TWR), allowing precise distance estimation between the anchor and each tag. In the anchor, the dual-antenna design enables phase-based AoA measurements, used to estimate the azimuth angle of incoming signals.

A preliminary calibration step is required for each mobile node to ensure accurate ranging. The procedure involves flashing the *UCI firmware* onto the tags, followed by calibration using the *Qorvo One TWR* graphical tool. The resulting parameters are saved in the non-volatile memory of the device.

After calibration, the nodes are flashed with a *Command-Line Interface (CLI) firmware* that allows the devices to operate in real-time measurement mode. Communication with the host computer occurs over USB, using a virtual serial interface to exchange commands and measurement packets.

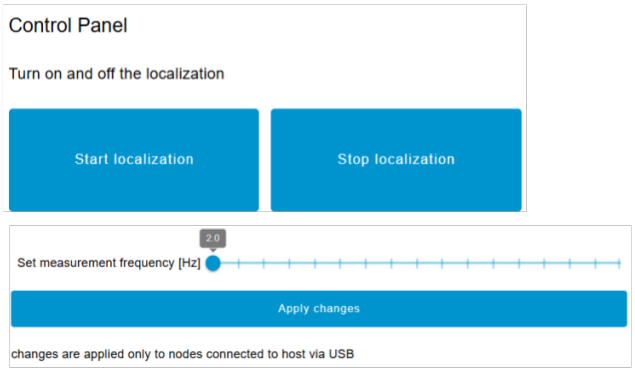

Fig. 2: Control panel for setting localization parameters.

All hardware setup and firmware procedures follow the standard steps described in Qorvo's Quick Start Guide and SDK documentation [12].

V. Software Architecture and Implementation

Most of the developed software logic is implemented in a Node-RED flow [19], which orchestrates data acquisition, processing, visualization, and control. A Node-RED Dashboard 2.0 [20] interface provides an interactive front-end for system configuration and monitoring.

A. Control Interface and Measurement Configuration

The system communicates with the UWB devices using a virtual serial interface over USB. The serial communication is managed within Node-RED through the use of the `node-red-node-serialport` package, which enables reading from and writing to multiple connected devices simultaneously.
Each UWB node (both anchor and tags) is flashed with a Command Line Interface (CLI) firmware that exposes a set of textual commands over the serial interface. These commands allow the configuration of measurement parameters, as well as starting and stopping ranging operations.

1) Centralized Configuration via Dashboard: The control interface is accessible in a Node-RED Dashboard panel depicted in Fig. 2, which allows the user to:

- Set the ranging period (i.e., measurement frequency) via a slider component.
- Initialize all nodes with the updated parameters.
- Start or stop measurement collection.

Pressing the *"Apply changes"* button in the dashboard triggers the communication of a series of CLI commands to each device. In order to update a devices it must be connected to the host machine during this setup phase. Note that different measuring frequency between the initiator (anchor) and responder (tags) could cause measurements to be unsuccessful.

The anchor node is initialized with the following command:

```
INITF -BLOCK=period -ADDR=0 -MULTI
-PADDR=[1,2,3,...]
```

Here, `ADDR=0` assigns the device as the anchor, `PADDR` defines the address list of tags to track (matches the ADDR of the responders), and `period` is the measurement interval (in ms), determined by the dashboard slider.

Each tag is configured as a responder using the command:

```
RESPF -BLOCK=period -ADDR=n -MULTI
-PADDR=0
```

where `n` is the unique address of the tag, and `PADDR=0` indicates that the anchor is the requesting device.

After initialization, devices are sent the following additional commands:

```
STOP
SAVE
```

These commands stop any running measurement session and save the configuration to non-volatile memory.

Moreover, by the commands `SAVEAPP INITF` and `SAVEAPP RESPF`, the applications (`INITF` and `RESPF`, respectively) are set as default, so that at each power-up they are automatically executed. Apart from configuring the frequency of measurement, tags are not required to be connected to host device. This allow the system to be plug-and-play.

2) Measurement Start/Stop: Once configured, measurements can be started and stopped using an additional dashboard button, which triggers the corresponding CLI commands to begin (`INITF`) or halt (`STOP`) real-time ranging and angle estimation to the anchor node. Note that to individually stop a tag from executing its application, it must be powered off.

B. Data Acquisition and Processing

1) Measurement Parsing: To extract meaningful measurement data from the incoming serial stream, a *Node-RED function node* contains a regular expression to parse each line. This function identifies valid measurement entries by matching specific fields provided by the Qorvo CLI firmware: `mac_address`, `distance[cm]`, `loc_az_pdoa`, `loc_az`, and `RSSI[dBm]`.

Once a match is found, the function extracts the relevant fields, casts them to numeric data types, and constructs a structured message payload. This filtered and structured data is then forwarded through the Node-RED flow for further processing, ensuring that only valid and usable measurement entries are handled.

2) Kalman Filter Tracking: To obtain smoothed and robust position and velocity estimates from noisy and asynchronous ToF and AoA measurements, a simple KF scheme is applied for each of the tracked tags. The KF fuses real-time measurements over time to reduce the impact of noise and to reconstruct hidden states such as velocity.

a) System Model: The system is modeled using a constant-velocity kinematic model in 2D. The state vector is defined as:

$$\mathbf{x}_k = \begin{bmatrix} x_k & y_k & \dot{x}_k & \dot{y}_k \end{bmatrix}^\top \tag{1}$$

Where x_k, y_k are the tag positions, and $\dot{x}_k, \dot{y}_k$ are the velocities. Tags positions are indicated in the reference frame as in Fig. 1.

The discretized dynamics is:

$$\mathbf{x}_{k+1} = \mathbf{A}\,\mathbf{x}_k + \mathbf{G}\,\mathbf{w}_k$$

where $\mathbf{w}_k \sim \mathcal{N}(0, \mathbf{Q})$ is zero-mean Gaussian process noise with covariance matrix $\mathbf{Q} = diag(\sigma_p^2, \sigma_p^2, \sigma_v^2, \sigma_v^2)$, and the system matrices are defined as:

$$\mathbf{A} = \begin{bmatrix} 1 & 0 & \Delta t & 0 \\ 0 & 1 & 0 & \Delta t \\ 0 & 0 & 1 & 0 \\ 0 & 0 & 0 & 1 \end{bmatrix}, \quad \mathbf{G} = \begin{bmatrix} \Delta t & 0 & \frac{1}{2}\Delta t^2 & 0 \\ 0 & \Delta t & 0 & \frac{1}{2}\Delta t^2 \\ 1 & 0 & \Delta t & 0 \\ 0 & 1 & 0 & \Delta t \end{bmatrix}$$

b) Measurement Model: The measurement vector at each time step includes the estimated distance and azimuth angle:

$$\mathbf{z}_k = \begin{bmatrix} \rho_k \\ \theta_k \end{bmatrix} = \mathbf{H}\mathbf{x}_k + \mathbf{v}_k$$

Where $\mathbf{v}_k \sim \mathcal{N}(0, \mathbf{R})$ is the measurement noise with covariance matrix $\mathbf{R} = diag(\sigma_\rho^2, \sigma_\theta^2)$. Since the measurement models are non-linear the Jacobian is computed according to the theory of the Extended KF (EKF) [21]:

$$\mathbf{H} = \begin{bmatrix} \frac{x_k}{D} & \frac{y_k}{D} & 0 & 0 \\ -\frac{y_k}{D^2} & \frac{x_k}{D^2} & 0 & 0 \end{bmatrix}, \quad \text{where } D = \sqrt{x_k^2 + y_k^2}$$

c) Kalman Filter Scheme: At initialization the estimates are initialized stationary in a random position and are assigned with huge uncertainty. After initialization the KF operates in real-time alternating predictions and updates.

- **Initialization**

$$\hat{\mathbf{x}}_0 = \begin{bmatrix} 1 & 1 & 0 & 0 \end{bmatrix}^\top$$
$$\mathbf{P}_0 = 10^4\ \mathbf{I}_4$$

where $\mathbf{I}_4$ is the identity matrix of dimension 4.

- **Prediction Step**

$$\hat{\mathbf{x}}_k^- = \mathbf{A}\hat{\mathbf{x}}_{k-1}$$
$$\mathbf{P}_k^- = \mathbf{A}\mathbf{P}_{k-1}\mathbf{A}^\top + \mathbf{G}\mathbf{Q}\mathbf{G}^\top$$

- **Update Step**

$$\mathbf{K}_k = \mathbf{P}_k^-\mathbf{H}^\top(\mathbf{H}\mathbf{P}_k^-\mathbf{H}^\top + \mathbf{R})^{-1}$$
$$\hat{\mathbf{x}}_k = \hat{\mathbf{x}}_k^- + \mathbf{K}_k(\mathbf{z}_k - \mathbf{H}\hat{\mathbf{x}}_k^-)$$
$$\mathbf{P}_k = (\mathbf{I}_4 - \mathbf{K}_k\mathbf{H})\mathbf{P}_k^-$$

The Kalman Filter operates continuously as new measurements arrive, correcting the state estimate and maintaining a smooth trajectory even under noisy or missing data. This approach is particularly effective in real environments where reflections, multi-path, and occlusions may affect the quality of individual range or angle estimates.

Real-time tracked positions are visualized on a Node-RED dashboard (Fig. 3), accompanied by measurement quality indicators such as a histogram of time intervals between consecutive measurements and the received signal strength (RSSI).

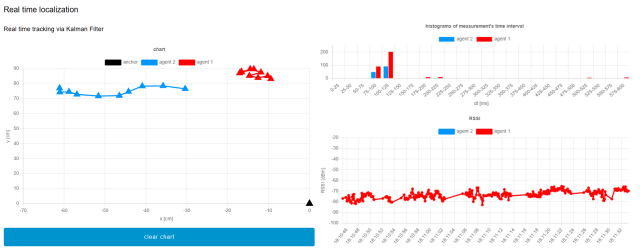

Fig. 3: Real-time plots for trajectory and signal quality metrics. On the left the 2D estimated positions of two tags are plotted. On the top-right an histogram of the measurement interval, while on the bottom the RSSI is plotted over time.

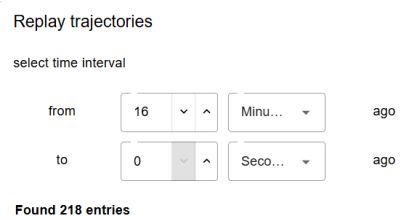

Fig. 4: Dashboard panel for selecting the replay time-window.

C. Storage and replay mode

To enable offline analysis and replay modes the filtered position estimates are persistently stored in a time-series database. The chosen backend is InfluxDB 2.0 [22], which provides optimized support for timestamped data, efficient querying, and easy integration with Node-RED.

1) Storage Pipeline: Each estimated position is sent from the Kalman Filter block in Node-RED to InfluxDB using a dedicated function node. The message payload includes the agent ID, cartesian coordinates, and signal quality indicator (RSSI). This data is stored in a dedicated *InfluxDB bucket* named `tracking`, under the measurement `estpos`. Each entry is automatically timestamped upon arrival, ensuring consistent chronological ordering.

While only the filtered estimates are used in the main system pipeline, a secondary bucket stores raw position estimates computed from individual ToF and AoA values without filtering. This dataset is reserved for validation and comparison purposes during the experimental phase and is not exposed through the user interface.

2) Replay Mode Querying: To allow visualization of past trajectories, a dedicated dashboard interface allows the user to specify a time window for retrieval. This is implemented using two numerical inputs and dropdowns in Dashboard 2.0 (Fig. 4), where the user selects the time offset (e.g., from "18 minutes ago" to "0 seconds ago"). These values are converted to timestamps by a function node.

To retrieve past data for visualization in the selected time interval, the following *Flux* query is executed within Node-RED to extract filtered positions from the `tracking` bucket:

```
from(bucket: "tracking")
  |> range(start: <startTime>, stop: <stopTime>)
  |> filter(fn: (r) => r._measurement == "estpos")
  |> filter(fn: (r) => r._field == "x" or r._field == "y" or r._field == "agent")
  |> pivot(rowKey:["_time"], columnKey: ["_field"], valueColumn: "_value")
  |> filter(fn: (r) => r.agent == "agent_1" or r.agent == "agent_2")
```

This query selects all position entries (`x`, `y`) and agent labels recorded in the bucket "tracking" within the user-defined time range. The use of the `pivot` operation reorganizes the data into a tabular format where each row contains a full position sample (timestamp, `x`, `y`, `agent`).

To ensure the clarity of visualizations during replay mode, especially when large time intervals are selected, the system allows the user to set a maximum number of points to be displayed on the dashboard. This avoids clutter and improves interpretability. This result is obtained by uniformly downsampling the full set of positions available within the selected interval, so that only a subset of evenly spaced samples (up to the specified limit) is plotted.

VI. System Validation and Performance Assessment

A. Validation Campaign

The validation campaign is performed by simultaneously localizing the tags w.r.t. the anchor using the designed system and using a marker-based Motion Capture (MoCap) system. The used MoCap system from Qualisys comprises of 8 different cameras positioned all around the room, capable of recording high-resolution videos and of measuring $3D$ positions of the markers triangulating over the reflected infrared light.
The calibrated MoCap system achieves sub-millimeter accuracy in position triangulation and is therefore considered as ground-truth, since the developed tracking system exhibits errors several orders of magnitude higher.

To obtain 6D poses (x, y, z coordinates and roll, pitch, yaw orientations) of each rigid body (tags and anchor), reflective markers were attached to the devices. Their placement was carefully designed to be asymmetric and sufficiently diverse to avoid ambiguities in rigid-body identification. Correct tracking requires at least 3 markers to be visible by two or more cameras per frame. To mitigate occlusions and ensure reliable tracking even away from the center of the room, additional markers were mounted.

The analysis was conducted by manually moving the two tags within the environment, positioning one closer to the anchor and the other further away to highlight performance differences. Measurements frequency was set at the maximum of 10Hz to get the best performance available. Furthermore, results are evaluated both against the estimates produced by the Kalman Filter and against the Raw Measurements (RM), thereby illustrating the necessity of the filtering layer.

After parsing the measured data, some processing operations are required. In fact, the MoCap data needs to be converted from $6D$ to $2D$ data by reprojecting coordinates to the space observable by the sensor.
First the distance d^i and angle θ^i between tags $i = 1, 2$ and anchor a is computed for each measurement k:

$$d_k^i = \sqrt{(x_k^i - x_k^a)^2 + (y_k^i - y_k^a)^2 + (z_k^i - z_k^a)^2}$$
$$\theta_k^i = atan\left(\frac{y_k^i - y_k^a}{x_k^i - x_k^a}\right) - \theta_z^a$$

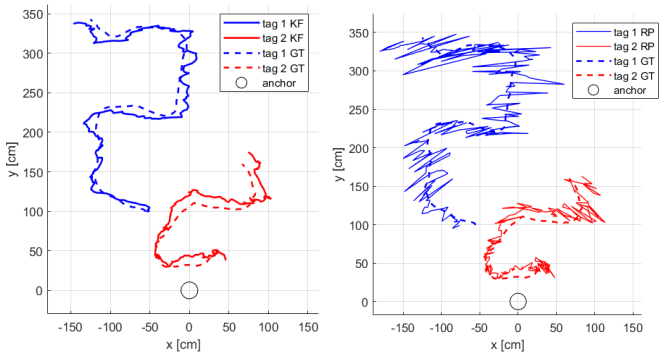

Fig. 5: $2D$ trajectories from KF (left) estimates and from Raw Measurements (right), against Ground Truth (GT).

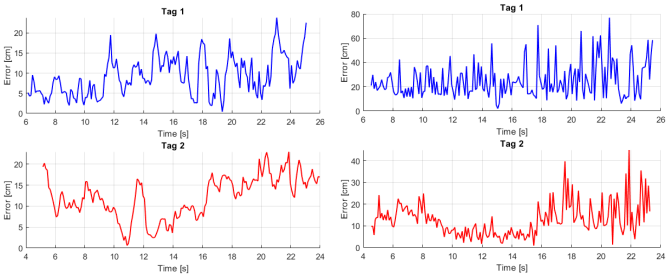

Fig. 6: Tracking error from KF estimates (left) and from Raw Measurements (right).

where θ_z^a is the rotation of the anchor reference frame from the global reference frame along the z axis. Note that the local z axis of the anchor correspond to the global z axis.
Then the distances and angles are converted to $2D$ coordinates to match the sensor reference frame:

$$\tilde{x}_k^i = d_k^i sin(\theta_k^i)$$
$$\tilde{y}_k^i = d_k^i cos(\theta_k^i)$$

Finally the tracking error ϵ_k^i can be computed as the norm of the difference between $(\tilde{x}^i, \tilde{y}^i)$ and $(x^{\mathrm{KF},i}, y^{\mathrm{KF},i})$ which are the estimates provided by the KF:

$$\epsilon_k^i = \sqrt{(x_k^{\mathrm{KF},i} - \tilde{x}_k^i)^2 + (y_k^{\mathrm{KF},i} - \tilde{y}_k^i)^2}$$

Similarly the tracking error is computed against the $2D$ coordinates obtained from Raw Measurements $(x^{\mathrm{RM},i}, y^{\mathrm{RM},i})$.

B. Experimental Results

In Fig. 5, the Kalman Filter estimates, despite being imprecise, yield a much smoother trajectory compared to the raw measurements. This observation is further supported by the tracking errors reported in Fig. 6.
The analysis of Tab. I reports how through Kalman Filtering the average tracking error is reduced by about 60% for tag 1, while for tag 2 the improvement is more modest, around 5%. From Fig. 5 it can be observed that, although the trajectory of tag 2 is smoothed, it exhibits a consistent offset from the ground truth, likely due to the close proximity to the anchor. Additional error metrics, including Root Mean Square Error, standard deviation, and the 95th percentile, show systematic

Metric	Tag 1 [cm]		Tag 2 [cm]	
	KF	RM	KF	RM
Avg. error	9.3	24.7	12.2	12.7
RMSE	10.4	28.4	13.2	14.8
Std. deviation	4.8	14.0	5.0	7.5
95th percentile	18.5	55.1	19.8	26.3

TABLE I: Tracking error metrics comparing Kalman Filter (KF) estimates and Raw Measurements (RM) for both tags. Values are reported in centimeters. KF generally reduces error and variance, particularly for Tag 1.

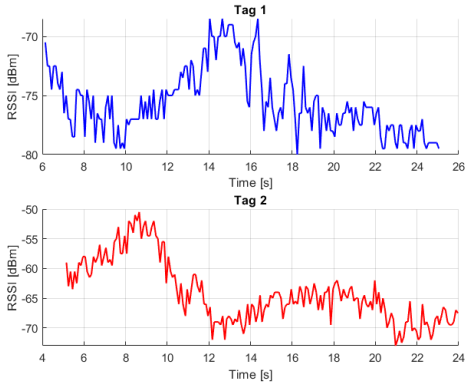

Fig. 7: Radio Signal Strength Indicator of UWB measurements.

reductions under filtering, reinforcing the hypothesis that a persistent bias, rather than random noise, is the dominant source of error.

As a final check, the Radio Signal Strength Indicator (RSSI), shown in Fig. 7, shows no evident correlation with the tracking error, suggesting that RSSI does not significantly influence the localization accuracy in the present setup.

VII. Conclusions

This work has demonstrated that reliable tag localization can be achieved with a single-anchor UWB setup, reaching decimeter-level accuracy under realistic experimental conditions. A key finding is the central role of Kalman Filtering, which significantly improves accuracy and stability by reducing noise and mitigating random fluctuations in the raw measurements. The single-anchor configuration not only simplifies deployment by minimizing setup effort, but also shows that competitive performance does not necessarily require complex multi-anchor infrastructures.

Beyond the localization performance, the developed system includes practical tools that enhance usability and scalability. In particular, the integration of real-time visualization through Node-RED and long-term data storage in InfluxDB provides an effective framework for monitoring, analysis, and future extensions. These results confirm both the technical feasibility and practical applicability of the proposed approach, making it a promising foundation for further research and real-world deployments.

References

[1] D. Wang, R. Kannan, L. Wei, and B. Tay, "Time of flight based two way ranging for real time locating systems," in *2010 IEEE Conference on Robotics, Automation and Mechatronics*, 2010, pp. 199–205.

[2] A. Florio, G. Avitabile, and G. Coviello, "Multiple source angle of arrival estimation through phase interferometry," *IEEE Transactions on Circuits and Systems II: Express Briefs*, vol. 69, no. 3, pp. 674–678, 2022.

[3] M. Delamare, R. Boutteau, X. Savatier, and N. Iriart, "Static and dynamic evaluation of an uwb localization system for industrial applications," *Sci*, vol. 2, no. 2, 2020. [Online]. Available: https://www.mdpi.com/2413-4155/2/2/23

[4] M. Kolakowski, "Improving accuracy and reliability of bluetooth low-energy-based localization systems using proximity sensors," *Applied Sciences*, vol. 9, no. 19, p. 4081, 2019.

[5] M. Kotaru, K. Joshi, D. Bharadia, and S. Katti, "Spotfi: Decimeter level localization using wifi," in *Proceedings of the 2015 ACM conference on special interest group on data communication*, 2015, pp. 269–282.

[6] H. S. Fahama, K. Ansari-Asl, Y. S. Kavian, and M. N. Soorki, "An experimental comparison of rssi-based indoor localization techniques using zigbee technology," *IEEE Access*, vol. 11, pp. 87 985–87 996, 2023.

[7] Q. Dong and W. Dargie, "Evaluation of the reliability of rssi for indoor localization," in *2012 International Conference on Wireless Communications in Underground and Confined Areas*, 2012, pp. 1–6.

[8] F. Riz, L. Palopoli, and D. Fontanelli, "Analysis of indistinguishable trajectories of a nonholonomic vehicle subject to range measurements," *IEEE Transactions on Automatic Control*, 2024.

[9] ——, "Why three measurements are not enough for trilateration-based localisation," in *2023 IEEE International Instrumentation and Measurement Technology Conference (I2MTC)*. IEEE, 2023, pp. 01–06.

[10] S. Zhao and D. Zelazo, "Bearing rigidity and almost global bearing-only formation stabilization," *IEEE Transactions on Automatic Control*, vol. 61, no. 5, pp. 1255–1268, 2015.

[11] A. Martinelli and R. Siegwart, "Observability analysis for mobile robot localization," in *2005 IEEE/RSJ International Conference on Intelligent Robots and Systems*. IEEE, 2005, pp. 1471–1476.

[12] Qorvo, Inc., "QM33120WDK1 Ultra-Wideband (UWB) Transceiver Development Kit," https://www.qorvo.com/products/p/QM33120WDK1, 2025, accessed: 2025-07-31.

[13] G. Miraglia, K. N. Maleki, and L. R. Hook, "Comparison of two sensor data fusion methods in a tightly coupled uwb/imu 3-d localization system," in *2017 International Conference on Engineering, Technology and Innovation (ICE/ITMC)*, 2017, pp. 611–618.

[14] L. Yao, Y.-W. A. Wu, L. Yao, and Z. Z. Liao, "An integrated imu and uwb sensor based indoor positioning system," in *2017 International Conference on Indoor Positioning and Indoor Navigation (IPIN)*, 2017, pp. 1–8.

[15] B. Großwindhager, M. Rath, J. Kulmer, M. S. Bakr, C. A. Boano, K. Witrisal, and K. Römer, "Salma: Uwb-based single-anchor localization system using multipath assistance," in *Proceedings of the 16th ACM Conference on Embedded Networked Sensor Systems*, 2018, pp. 132–144.

[16] Y. Cao, C. Yang, R. Li, A. Knoll, and G. Beltrame, "Accurate position tracking with a single uwb anchor," in *2020 IEEE International Conference on Robotics and Automation (ICRA)*, 2020, pp. 2344–2350.

[17] S. Roumeliotis and G. Bekey, "Distributed multirobot localization," *IEEE Transactions on Robotics and Automation*, vol. 18, no. 5, pp. 781–795, 2002.

[18] T. Wang, H. Zhao, and Y. Shen, "An efficient single-anchor localization method using ultra-wide bandwidth systems," *Applied Sciences*, vol. 10, no. 1, 2020. [Online]. Available: https://www.mdpi.com/2076-3417/10/1/57

[19] OpenJS Foundation & Contributors, "Node-RED," https://nodered.org, 2025.

[20] FlowFuse, "Node-RED Dashboard 2.0 (FlowFuse Dashboard)," https://dashboard.flowfuse.com, 2025.

[21] S. Konatowski, A. Pieni *et al.*, "A comparison of estimation accuracy by the use of kf, ekf & ukf filters," *WIT Transactions on modelling and simulation*, vol. 46, 2007.

[22] InfluxData, Inc., "InfluxDB OSS v2 (Time Series Platform)," https://docs.influxdata.com/influxdb/v2/, 2025, accessed: 2025-08-21.